symmetry

MDPI

Article

Influence of an External Classical Field on a ◊ Four-Level Atom Inside a Quantized Field

Eied Mahmoud Khalil [1], Hanaa Abu-Zinadah [2] and Mahmoud Youssef Abd-Rabbou [3,*]

[1] Department of Mathematics, College of Science, Taif University, P.O. Box 11099, Taif 21944, Saudi Arabia; eiedkhalil@yahoo.com
[2] Department of Statistics, College of Science, University of Jeddah, Jeddah 23218, Saudi Arabia; hhabuznadah@uj.edu.sa
[3] Mathematics Department, Faculty of Science, Al-Azhar University, Nasr City, Cairo 11884, Egypt
* Correspondence: m.elmalky@azhar.edu.eg

Abstract: In this paper, we study the effect of detuning parameters and driven external classical field parameters on a quantum system consisting of a ◊-configuration four-level atom inside a quantized cavity field. Under some canonical conditional of dressed states, the exact solution of the Schrödinger equation is obtained. The occupation of atomic levels and statistical population inversion is studied. Our results show that the classical field parameter dissolved the collapse periods and increased the maximum bounds of the upper state, while decreasing the lower bounds of the lower state. The detuning parameters reduce the minimum bounds of atomic levels and their inversion. On the other hand, the linear entropy and l_1 norm of coherence are employed to measure the temporal evolution of the mixedness and coherence. It is found that the driven classical field improves the temporal evolution of the mixedness and lower bounds of coherence. However, the detuning parameters have a destructive effect on the mixedness and lower bounds of coherence. The intensity of the external classical field is regarded as a control parameter with different values of detuning parameters.

Keywords: four-level atom; external classical field; mixedness; coherence

Citation: Khalil, E.M.; Abu-Zinadah, H.; Abd-Rabbou, M.Y. Influence of an External Classical Field on a ◊ Four-Level Atom Inside a Quantized Field. *Symmetry* **2022**, *14*, 811. https://doi.org/10.3390/sym14040811

Academic Editors: Vasilis K. Oikonomou, Ignatios Antoniadis and Ioan Raşa

Received: 3 March 2022
Accepted: 11 April 2022
Published: 14 April 2022

1. Introduction

The interaction between a quantized field and atomic state is one of the most attractive topics in quantum optics. The Rabi model is the first uncomplicated theoretical model that describes a direct interaction between a single quantized photon and a two-level atom [1]. Another theoretical model that has opened the way for numerous experimental and theoretical quantum studies is called the Jaynes–Cummings model (JCM), which is solved under the rotating wave approximation technique [2]. Overall, the generalization of atom–field interaction has been demonstrated in many theoretical studies, e.g., the interaction between an optical electromagnetic field and N-level atomic stat has been investigated [3,4]. The resonance and non-resonance cases of multi-photon JCM have been discussed [5]. Moreover, high-dimensional atomic states inside an electromagnetic field have been widely studied. For example, the quantum correlation and some statistical characteristics of the three-level atom, four-level atom, and five-level atom have been explored [6–8]. Additionally, the influence of some external effects on atom–field interaction has been proposed, such as Kerr-like medium [9,10], vibrating graphene membrane [11,12], external classical field [13–15], and deformed fields [16,17]. In particular, the interaction between a four-level atom and different types of a cavity mode field has been paid more attention under different configurations [18–22]. The effect of external classical fields in the two-level atom scheme coupled with a quantized electromagnetic field was studied [13]. The squeezing phenomenon and entanglement of JCM in the presence of driven classical field has been discussed [23]. In SU(1,1) Lie algebra, the influence of the off-resonance case

and driven classical field on a Λ configuration three-level atom interacting with SU(1,1) Lie algebra has been displayed [24].

The degree of entanglement is one of the outstanding properties of quantum states, which may be evaluated via different measurements. The quantum concurrence and negativity are regarded as the best quantifiers of entanglement for finite dimensions [25,26]. The time evolution of entanglement in the presence of Kerr-like medium [27], driven laser field [28], intrinsic decoherence [29], a classical homogeneous gravitational field [7], and Stark-shift [30] has been investigated. Based on quantum information theory, an optimal scheme to quantify the degree of quantum coherence [31] has been reconstructed. In general, the behavior of coherence measurement may be used either as an entropic or metric measure such as Jensen–Shannon divergence [32], the geometric measure of coherence [33], the relative quantum of coherence [31], and the coherence of formation [34].

This study is motivated by the effect of an external classical field parameter on a ◊ four-level atom inside a quantized field. In the presence of an external classical field, solving a four-level atom needs many approximations [35]. In our solution, we have used some canonical transformations to solve the Hamiltonian. Moreover, this model and these results are interesting, and will be useful for future experiments, such as studying the process of four-wave mixing, both theoretically and experimentally for a ◊-configuration four-level atomic system [36]. Experimental observation of a tripod configuration for a four-level atom has been used to improve the cross-phase modulation based on a double electromagnetically induced transparency [37]. A new technique is proposed to solve the Hamiltonian physical model, where the classical field associates the two intermediate states together and simultaneously associates the upper state with the lower state. The statistical aspects and quantum correlation of this system is still an effective topic in experimental and theoretical schemes.

The paper is organized as follows: in Section 2, the description of the physical model and its exact solution is presented, in which we obtain the temporal wave function. Consequently, the final atomic density state and the occupation of atomic levels are obtained. Section 3 investigates the temporal evolution of statistical inversion under the influence of driven classical field. The optimal behavior of the mixedness and purity via linear entropy, and the temporal evolution of coherence via the l_1 norm are discussed in Sections 4 and 5. Finally, Section 6 displays our conclusions.

2. Description of the Physical Model

Let us assume that a physical system consists of a single ◊ configuration of a four-level atom inside a single mode of a quantized field and simultaneously driven by an external classical laser field. As schematically shown in Figure 1, the permitted transitions between the atomic levels are $|1\rangle \mapsto \{|2\rangle, |3\rangle\}$, and $\{|2\rangle, |3\rangle\} \mapsto |4\rangle$, where $|1\rangle, |4\rangle$ are the top and ground state, while $|2\rangle, |3\rangle$ are the two intermediate states. The classical field associates the two intermediate states together and simultaneously associates the upper state with the lower state. The Hamiltonian that describes this system under the rotating wave approximation is written as ($\hbar = 1$),

$$\hat{H} = \hat{H}_{free} + \hat{H}_{int} + \hat{H}_{driven}, \tag{1}$$

where

$$\begin{aligned} \hat{H}_{free} &= \omega_f \hat{a}^\dagger \hat{a} + \sum_{i=1}^{4} \omega_i \hat{\sigma}_{ii}, \\ \hat{H}_{int} &= \lambda_1 \left(\hat{a}(\hat{\sigma}_{12} + \hat{\sigma}_{13} + \hat{\sigma}_{24} + \hat{\sigma}_{34}) + h.c. \right), \\ \hat{H}_{driven} &= \lambda_2 (\hat{\sigma}_{14} + \hat{\sigma}_{23} + h.c.) \end{aligned} \tag{2}$$

where ω_f and ω_i are the frequencies of the field and atomic transition, respectively, λ_1 and λ_2 donate the coupling of the strength atom field and external field, respectively. $\hat{a}$ donates the bosonic annihilation of the quantized field with the Hermitian conjugate $\hat{a}^\dagger$

which satisfies $[\hat{a}, \hat{a}^\dagger] = I$, and $\hat{\sigma}_{ij} = |i\rangle\langle j|$ are the atomic raising operators with the lowering operator $\hat{\sigma}_{ji} = |j\rangle\langle i|$.

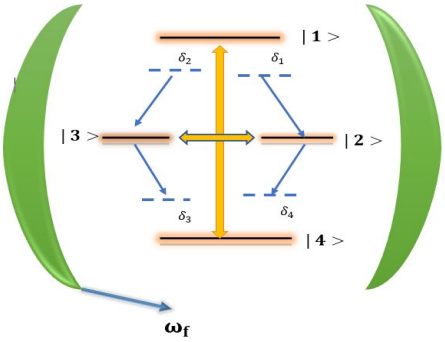

Figure 1. A sketch of a ◊ configuration of a four-level atom inside a cavity field influenced by the classical field. Here, ω_f is the frequency of the quantized field. The classical field is represented by the transition from $|1\rangle$ to $|4\rangle$ and from $|2\rangle$ to $|3\rangle$.

Via denationalization for the free atomic subsystem $\sum_{i=1}^{4} \omega_i \hat{\sigma}_{ii}$ and the driven Hamiltonian $\hat{H}_{driven}$, one can obtain the following eigenstates:

$$\begin{aligned} |1\rangle &= \cos\frac{\zeta_1}{2}|e\rangle - \sin\frac{\zeta_1}{2}|g\rangle, \qquad |2\rangle = \cos\frac{\zeta_2}{2}|i\rangle - \sin\frac{\zeta_2}{2}|f\rangle, \\ |3\rangle &= \cos\frac{\zeta_2}{2}|f\rangle + \sin\frac{\zeta_2}{2}|i\rangle, \qquad |4\rangle = \cos\frac{\zeta_1}{2}|g\rangle + \sin\frac{\zeta_1}{2}|e\rangle, \\ \zeta_1 &= \arctan\frac{2\lambda_2}{\omega_1 - \omega_4} \qquad \zeta_2 = \arctan\frac{2\lambda_2}{\omega_2 - \omega_3} \end{aligned} \tag{3}$$

where the atomic states $|1\rangle$, $|2\rangle$, $|3\rangle$, $|4\rangle$ are transformed under the above conditional dressed state to $|e\rangle$, $|i\rangle$, $|f\rangle$, $|g\rangle$. Therefore, the total physical Hamiltonian (1) in the dressed states (3) may be written as

$$\hat{\mathcal{H}} = \omega_f \hat{a}^\dagger \hat{a} + \Omega_1 \hat{S}_{ee} + \Omega_2 \hat{S}_{ii} + \Omega_3 \hat{S}_{ff} + \Omega_4 \hat{S}_{gg} + \hat{a}\left(\Lambda_1 \hat{S}_{ei} + \Lambda_2 \hat{S}_{ef} + \Lambda_3 \hat{S}_{ig} + \Lambda_4 \hat{S}_{fg}\right) + h.c., \tag{4}$$

with

$$\hat{S} = |r\rangle\langle s|, \; r, s = e, i, f, g. \tag{5}$$

Now, the atomic transitions are given by

$$\begin{aligned} \Omega_1 &= \omega_1 \cos^2\frac{\zeta_1}{2} + \omega_2 \sin^2\frac{\zeta_1}{2} + \lambda_2 \sin\zeta_1, \quad \Omega_2 = \omega_2 \cos^2\frac{\zeta_2}{2} + \omega_3 \sin^2\frac{\zeta_2}{2} + \lambda_2 \sin\zeta_2, \\ \Omega_3 &= \omega_3 \cos^2\frac{\zeta_2}{2} + \omega_2 \sin^2\frac{\zeta_2}{2} - \lambda_2 \sin\zeta_2, \quad \Omega_4 = \omega_4 \cos^2\frac{\zeta_1}{2} + \omega_1 \sin^2\frac{\zeta_1}{2} - \lambda_2 \sin\zeta_1, \end{aligned} \tag{6}$$

Meanwhile, the coupling strengths are obtained by

$$\begin{aligned} \Lambda_1 &= \cos\frac{\zeta_1 - \zeta_2}{2} + \sin\frac{\zeta_1 + \zeta_2}{2}, \quad \Lambda_2 = \cos\frac{\zeta_1 + \zeta_2}{2} + \sin\frac{\zeta_1 - \zeta_2}{2}, \\ \Lambda_3 &= \cos\frac{\zeta_1 + \zeta_2}{2} - \sin\frac{\zeta_1 - \zeta_2}{2}, \quad \Lambda_4 = \cos\frac{\zeta_1 - \zeta_2}{2} - \sin\frac{\zeta_1 + \zeta_2}{2}. \end{aligned} \tag{7}$$

By applying the Heisenberg equation of motion, the physical Hamiltonian (4) can be written as

$$\hat{\mathcal{H}} = \omega_f \mathcal{N} + \Omega_1 \mathcal{I} + \mathcal{H}_{int}, \tag{8}$$

Here, $\mathcal{I} = \sum_{r=1} \hat{S}_{rr}$, $\mathcal{N} = \hat{a}^\dagger \hat{a} - \hat{S}_{ii} - \hat{S}_{ff} - 2\hat{S}_{gg}$, and the interaction Hamiltonian $\mathcal{H}_{int}$ is obtained by

$$\mathcal{H}_{int} = \begin{bmatrix} 0 & \Lambda_1\hat{a} & \Lambda_2\hat{a} & 0 \\ \Lambda_1\hat{a}^\dagger & \delta_1 & 0 & \Lambda_3\hat{a} \\ \Lambda_2\hat{a}^\dagger & 0 & \delta_2 & \Lambda_4\hat{a} \\ 0 & \Lambda_3\hat{a}^\dagger & \Lambda_4\hat{a}^\dagger & \delta_3 \end{bmatrix} \tag{9}$$

with $\delta_1 = \omega + \Omega_2 - \Omega_1$, $\delta_2 = \omega + \Omega_3 - \Omega_1$, and $\delta_3 = 2\omega + \Omega_4 - \Omega_1$.

To investigate the effect of the external field, we shall obtain the exact solution of the wavefunction $|\psi(t)\rangle$ associated with the interaction Hamiltonian (9), which takes the form

$$|\psi(t)\rangle = \sum_{n=0}^{\infty} \Big(\mathcal{A}_1(n,t)|n,e\rangle + \mathcal{A}_2(n+1,t)|n+1,i\rangle + \mathcal{A}_3(n+1,t)|n+1,f\rangle + \mathcal{A}_4(n+2,t)|n+2,g\rangle \Big). \tag{10}$$

Altogether, the time-dependent Schrödinger equation $i\frac{\partial}{\partial t}|\psi(t)\rangle = \mathcal{H}_{int}|\psi(t)\rangle$ leads to a system of four ordinary differential equations:

$$\begin{aligned}
i\frac{\partial \mathcal{A}_1(n,t)}{\partial t} &= \nu[n]\big(\Lambda_1\mathcal{A}_2(n+1,t) + \Lambda_2\mathcal{A}_3(n+1,t)\big), \\
i\frac{\partial \mathcal{A}_2(n+1,t)}{\partial t} &= \delta_1\mathcal{A}_2(n+1,t) + \nu[n]\Lambda_1\mathcal{A}_1(n,t) + \nu[n+1]\Lambda_3\mathcal{A}_4(n+2,t)\big), \\
i\frac{\partial \mathcal{A}_3(n+1,t)}{\partial t} &= \delta_2\mathcal{A}_3(n+1,t) + \nu[n]\Lambda_2\mathcal{A}_1(n,t) + \nu[n+1]\Lambda_4\mathcal{A}_4(n+2,t)\big), \\
i\frac{\partial \mathcal{A}_4(n+2,t)}{\partial t} &= \delta_3\mathcal{A}_4(n+2,t) + \nu[n+1]\big(\Lambda_3\mathcal{A}_2(n+1,t) + \Lambda_4\mathcal{A}_3(n+1,t)\big),
\end{aligned} \tag{11}$$

where $\nu[n] = \lambda_1\sqrt{n+1}$. Now, we assume that the initial atomic state is initially prepared in the upper state, while the field is initially prepared in the coherent state $|\alpha\rangle$ with

$$|\alpha\rangle = \sum_{n=0}^{\infty} z_n|n\rangle, \quad z_n = \frac{\alpha^n}{\sqrt{n!}}e^{-\frac{|\alpha|^2}{2}}. \tag{12}$$

The exact solution of the time-dependence of probability amplitudes in differential Equations (11) by employing the Laplace transform method is given by

$$\begin{bmatrix} \mathcal{A}_1(n,t) \\ \mathcal{A}_2(n+1,t) \\ \mathcal{A}_3(n+1,t) \\ \mathcal{A}_4(n+2,t) \end{bmatrix} = \begin{bmatrix} f_{11} & f_{12} & f_{13} & f_{14} \\ f_{21} & f_{22} & f_{23} & f_{24} \\ f_{31} & f_{32} & f_{33} & f_{34} \\ f_{41} & f_{42} & f_{43} & f_{44} \end{bmatrix} \begin{bmatrix} e^{\eta_1 t} \\ e^{\eta_2 t} \\ e^{\eta_3 t} \\ e^{\eta_4 t} \end{bmatrix} \tag{13}$$

where

$$\begin{bmatrix} f_{1j} \\ f_{2j} \\ f_{3j} \\ f_{4j} \end{bmatrix} = \frac{z_n}{\eta_{ji}\eta_{jk}\eta_{jl}} \begin{bmatrix} q_1 + \eta_j(q_2 + \eta_j(q_3 + \eta_j)) \\ w_1 + \eta_j(w_2 + \eta_j w_3) \\ e_1 + \eta_j(e_2 + \eta_j e_3) \\ r_1 + \eta_j r_2 \end{bmatrix} \text{with } \eta_{jk} = \eta_j - \eta_k,\ i \neq j \neq k \neq l = 1,2,3,4 \tag{14}$$

with

$$\begin{aligned}
&\eta_{1,2} = \chi^- \pm \tau^- \quad \eta_{3,4} = \chi^+ \pm \tau^+, \qquad \chi^\pm = \frac{-x_1}{4} \pm \frac{y_1}{2}, \quad \tau^\pm = \frac{1}{2}\sqrt{y_2 \pm \frac{y_3}{4y_1}}, \\
&y_1 = \sqrt{g_1 + \frac{g_2}{3g_3} + \frac{g_3}{3}}, \quad y_2 = 2g_1 - \frac{g_2}{3g_3} - \frac{g_3}{3}, \quad y_3 = 4x_1x_2 - x_1^3 - 8x_3, \\
&g_1 = \frac{x_1^2}{4} - \frac{2x_2}{3}, \quad g_2 = x_2^2 + 12x_4 - 3x_1x_3, \quad g_3 = \sqrt[3]{\frac{d + \sqrt{d^2 - 4g_2^3}}{2}}, \\
&\text{and } d = 2x_2^3 + 27(x_3^2 + x_1^2x^4) - 72x_2x_4 - 9x_1x_2x_3, \\
&x_1 = i(\delta_1 + \delta_2 + \delta_3), \quad x_2 = \nu_n^2[\Lambda_1^2 + \Lambda_2^2] + \nu_{n+1}^2[\Lambda_3^2 + \Lambda_4^2] - \delta_1(\delta_2 + \delta_3) - \delta_2\delta_3, \\
&x_3 = i\Big(\delta_1(\nu_n^2\Lambda_2^2 + \nu_{n+1}^2\Lambda_4^2 - \delta_2\delta_3) + \delta_2(\nu_n^2\Lambda_1^2 + \nu_{n+1}^2\Lambda_3^2) + \delta_3\nu_n^2(\Lambda_1^2 + \Lambda_2^2)\Big), \\
&x_4 = \nu_n^2\nu_{n+1}^2(\Lambda_1\Lambda_4 - \Lambda_2\Lambda_3)^2 - \delta_3\nu_n^2(\Lambda_1\delta_2 + \Lambda_2\delta_1).
\end{aligned} \tag{15}$$

Additionally,

$$\begin{aligned}
&q_1 = i(\nu_{n+1}^2(\Lambda_3^2\delta_2 + \Lambda_4^2\delta_1) - \delta_1\delta_2\delta_3), \quad q_2 = \nu_{n+1}^2(\Lambda_3^2 + \Lambda_4^2 - \delta_1(\delta_2 + \delta_3) - \delta_2\delta_3),\\
&q_3 = i(\delta_1 + \delta_2 + \delta_3), \quad w_1 = i\nu_n(\Lambda_1\delta_2\delta_3 + \nu_{n+1}^2\Lambda_4(\Lambda_2\Lambda_3 - \Lambda_1\Lambda_4)), \quad w_2 = \Lambda_1(\delta_2 + \delta_3),\\
&w_3 = -i\Lambda_1, \quad e_1 = i\nu_n(\Lambda_2\delta_1\delta_3 + \nu_{n+1}^2\Lambda_3(\Lambda_1\Lambda_4 - \Lambda_2\Lambda_3)), \quad e_2 = \Lambda_2(\delta_2 + \delta_3), \quad e_3 = -i\Lambda_2,\\
&r_1 = -i\nu_n\nu_{n+1}(\Lambda_1\Lambda_3\delta_2 + \Lambda_2\Lambda_4\delta_1), \qquad r_2 = -\nu_n\nu_{n+1}(\Lambda_1\Lambda_3 + \Lambda_2\Lambda_4).
\end{aligned} \tag{16}$$

The main task of this manuscript is to investigate the influence of the driven classical field on the behavior of the atomic inversion and quantum correlation. Therefore, it is important to obtain the reduced density operator of the four-level atom sub-state. To obtain the atomic sub-state, one traces out the field degree of freedom, i.e., $\hat{\rho}_A = Tr_{field}|\psi(t)\rangle\langle\psi(t)|$, where $|\psi(t)\rangle$ is defined in Equation (10). Therefore, the reduced density operator using the transformation (3) is given by

$$\hat{\rho}_A = \begin{bmatrix} \rho_{11} & \rho_{12} & \rho_{13} & \rho_{14} \\ \rho_{21} & \rho_{22} & \rho_{23} & \rho_{24} \\ \rho_{31} & \rho_{32} & \rho_{33} & \rho_{34} \\ \rho_{41} & \rho_{42} & \rho_{43} & \rho_{44} \end{bmatrix} \tag{17}$$

$$\begin{aligned}
\rho_{11} &= |\mathcal{A}_1^n(t)|^2\cos^2\frac{\zeta_1}{2} - Re[\mathcal{A}_1^{n+2}(t)\mathcal{A}_4^{n^*}(t)]\sin\zeta_1 + |\mathcal{A}_4^n(t)|^2\sin^2\frac{\zeta_1}{2},\\
\rho_{22} &= |\mathcal{A}_2^n(t)|^2\cos^2\frac{\zeta_2}{2} - Re[\mathcal{A}_2^n(t)\mathcal{A}_3^{n^*}(t)]\sin\zeta_2 + |\mathcal{A}_3^n(t)|^2\sin^2\frac{\zeta_2}{2},\\
\rho_{33} &= |\mathcal{A}_3^n(t)|^2\cos^2\frac{\zeta_2}{2} + Re[\mathcal{A}_2^n(t)\mathcal{A}_3^{n^*}(t)]\sin\zeta_2 + |\mathcal{A}_2^n(t)|^2\sin^2\frac{\zeta_2}{2},\\
\rho_{44} &= |\mathcal{A}_4^n(t)|^2\cos^2\frac{\zeta_1}{2} + Re[\mathcal{A}_1^{n+2}(t)\mathcal{A}_4^{n^*}(t)]\sin\zeta_1 + |\mathcal{A}_1^n(t)|^2\sin^2\frac{\zeta_1}{2},\\
\rho_{14} &= \frac{\sin^2\zeta_1}{2}(|\mathcal{A}_1^n(t)|^2 - |\mathcal{A}_4^n(t)|^2) - \mathcal{A}_1^{n+2}(t)\mathcal{A}_4^{n^*}(t)\sin^2\frac{\zeta_1}{2} + \mathcal{A}_1^{n+2^*}(t)\mathcal{A}_4^n(t)\cos^2\frac{\zeta_1}{2} = \rho_{41}^*,\\
\rho_{23} &= \frac{\sin^2\zeta_2}{2}(|\mathcal{A}_2^n(t)|^2 - |\mathcal{A}_3^n(t)|^2) - \mathcal{A}_3^n(t)\mathcal{A}_2^{n^*}(t)\sin^2\frac{\zeta_2}{2} + \mathcal{A}_3^{n^*}(t)\mathcal{A}_2^n(t)\cos^2\frac{\zeta_2}{2} = \rho_{32}^*,\\
\rho_{12} &= \left(\cos\frac{\zeta_1}{2}\mathcal{A}_1^{n+1}(t) - \sin\frac{\zeta_1}{2}\mathcal{A}_4^n(t)\right)\left(\mathcal{A}_2^{n^*}(t)\cos\frac{\zeta_2}{2} - \mathcal{A}_3^{n^*}(t)\sin\frac{\zeta_2}{2}\right) = \rho_{21}^*,\\
\rho_{13} &= \left(\cos\frac{\zeta_1}{2}\mathcal{A}_1^{n+1}(t) - \sin\frac{\zeta_1}{2}\mathcal{A}_4^n(t)\right)\left(\mathcal{A}_2^{n^*}(t)\cos\frac{\zeta_2}{2} + \mathcal{A}_3^{n^*}(t)\sin\frac{\zeta_2}{2}\right) = \rho_{31}^*,\\
\rho_{42} &= \left(\sin\frac{\zeta_1}{2}\mathcal{A}_1^{n+1}(t) + \cos\frac{\zeta_1}{2}\mathcal{A}_4^n(t)\right)\left(\mathcal{A}_2^{n^*}(t)\cos\frac{\zeta_2}{2} - \mathcal{A}_3^{n^*}(t)\sin\frac{\zeta_2}{2}\right) = \rho_{24}^*,\\
\rho_{43} &= \left(\sin\frac{\zeta_1}{2}\mathcal{A}_1^{n+1}(t) + \cos\frac{\zeta_1}{2}\mathcal{A}_4^n(t)\right)\left(\mathcal{A}_2^{n^*}(t)\cos\frac{\zeta_2}{2} + \mathcal{A}_3^{n^*}(t)\sin\frac{\zeta_2}{2}\right) = \rho_{34}^*,
\end{aligned} \tag{18}$$

Hereinafter, we shall employ the final reduced atomic density state to discuss some statistical properties and quantum correlation of the system.

First, we have investigated the occupation of atomic levels by a plot of the diagonal element of the final reduced density state (17). Figure 2 displays the effect of the detuning parameter and the coupling strength of the external classical field on the occupation of atomic levels when α = 5. The dynamical evolution of ρ_{11} (green-solid), ρ_{22} (blue-dot dash), ρ_{33} (red-dash), and ρ_{44}(black-dot) are represented in Figure 2a, where the coupling strength of classical field is zero ($\lambda_2 = 0$) and there are small values of the detunings $(\delta_1, \delta_2, \delta_3) = (\omega_f, 0.25\,\omega_f, \omega_f)$. It is clear that the populations of the levels ρ_{11} and ρ_{44} have symmetric behaviors. Likewise, the two intermediate states ρ_{22} and ρ_{33} are symmetric, but the upper bounds of the upper and lower states are frequently different to that depicted for the two intermediate density states.

Moreover, for the small strength of classical field $(\lambda_2 = 0.3)$ with detuning $(\delta_1, \delta_2, \delta_3) = (\omega_f, 0.25\,\omega_f, \omega_f)$, the collapse periods of upper and lower density states are removed, while the two intermediate density states are identical. As the detuning increases $(\delta_1, \delta_2, \delta_3) = (6\omega_f, 3\,\omega_f, 6\omega_f)$ and $(\lambda_2 = 0)$, the occupation of atomic levels are totally separated, the phenomena of collapse intervals disappears for ρ_{11}, ρ_{33}, and ρ_{44}. The upper bounds of ρ_{11}, ρ_{33} increase and the lower bounds of ρ_{44} decrease, while the distribution of ρ_{22} keeps his occupation. Figure 2d shows the effect of a small classical field $(\lambda_2 = 0.3)$ with $(\delta_1, \delta_2, \delta_3) = (6\omega_f, 3\,\omega_f, 6\omega_f)$. An increase in the fluctuation in the periods of collapse over the four levels is noted. For large values of detuning $(\delta_1, \delta_2, \delta_3) = (15\omega_f, 0.5\delta_1, 10\omega_f)$ and $(\lambda_2 = 0)$, Figure 2e depicts a decrease in the upper bounds of the atomic level occupation.

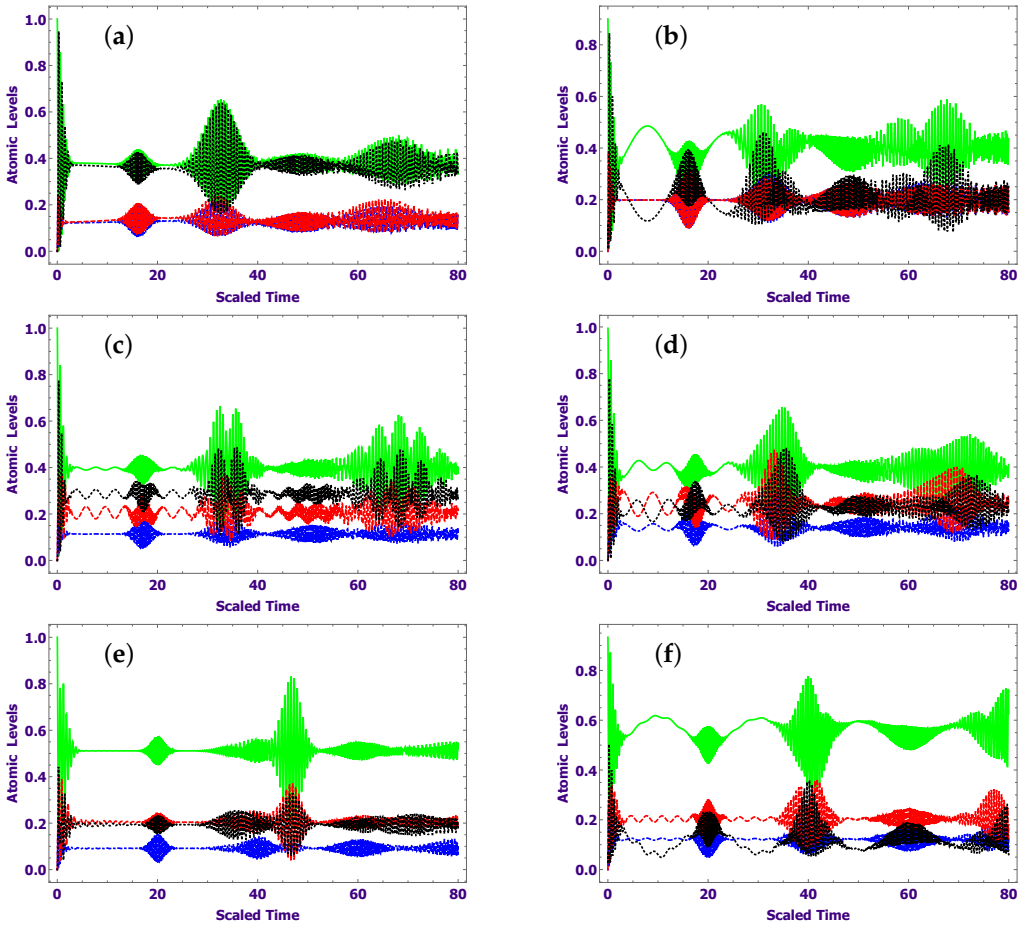

Figure 2. The influence of detuning and external field on the population of atomic levels ρ_{11}(green-solid), ρ_{22}(blue-dot dash), ρ_{33}(red-dash), and ρ_{44}(black-dot) with $\alpha = 5$. (**a**) $\delta_1 = \delta_3 = w$, $\delta_2 = 0.25\delta_1$, $\lambda_2 = 0$, (**b**) $\delta_1 = \delta_3 = w$, $\delta_2 = 0.25\delta_1$, $\lambda_2 = 0.3$, (**c**) $\delta_1 = \delta_3 = 6w$, $\delta_2 = 0.5\delta_1$, $\lambda_2 = 0$, (**d**) $\delta_1 = \delta_3 = 6w$, $\delta_2 = 0.5\delta_1$, $\lambda_2 = 0.3$, (**e**) $\delta_1 = 15\omega_f$ $\delta_2 = 0.5\delta_1$, $\delta_3 = 10\omega_f$, $\lambda_2 = 0$, (**f**) $\delta_1 = 15\omega_f$ $\delta_2 = 0.5\delta_1$, $\delta_3 = 10\omega_f$, $\lambda_2 = 2$.

The collapse interval increases, and the distribution of ρ_{33} and ρ_{44} has symmetric behavior. Finally, Figure 2f shows that the large strength of the classical field $(\lambda_2 = 2)$ and large detuning decreases the upper bounds of the occupation phenomena. The collapse periods disappear, and the lower state ρ_{44} is noticeably diminished.

3. Atomic Inversion

In this section, we discuss the influence of detuning and classical field parameters on the difference between the atomic levels by using the atomic inversion. It is defined by

$$\mathcal{W}(t) = \rho_{11} + \rho_{22} + \rho_{33} - \rho_{44}. \tag{19}$$

Under the same values of Figure 2, the effect of different values of detuning and the strength of the classical field on the statistical population inversion is displayed in Figure 3. As displayed in Figure 3a, the temporal evolution of statistical inversion fluctuates between negative and positive values, but the inversion has more positive values. This means that the energy of the upper state is larger than that existing in the lower state. After the onset interaction, the small strength of the classical field $(\lambda_2 = 0.3)$ dissolves the collapse periods. However, the negative values of revivals is transposed to positive values; therefore, the energy exchanges approach the upper state. As the detuning increases $(\delta_1, \delta_2, \delta_3) = (6\omega_f, 3\,\omega_f, 6\omega_f)$ and $(\lambda_2 = 0)$, Figure 3c shows that the upper bounds of the statistical population inversion increase after the onset interaction. The collapse intervals disappear, and the revival intervals fluctuate. By adding the classical field effect, the revival intervals are regulated, and the upper bounds of the inversion increase. For large detuning in the absence of the classical field effect, the statistical inversion shifts to non-negative values. This means that the energy approach to the upper state and the amplitude of revival periods are decreased. For a large strength of classical field and detuning, Figure 3f depicts that the collapse periods vanish. Since the occupation of ρ_{11} is higher than ρ_{44}, the upper bounds of statistical inversion increase to approach to the upper excited state.

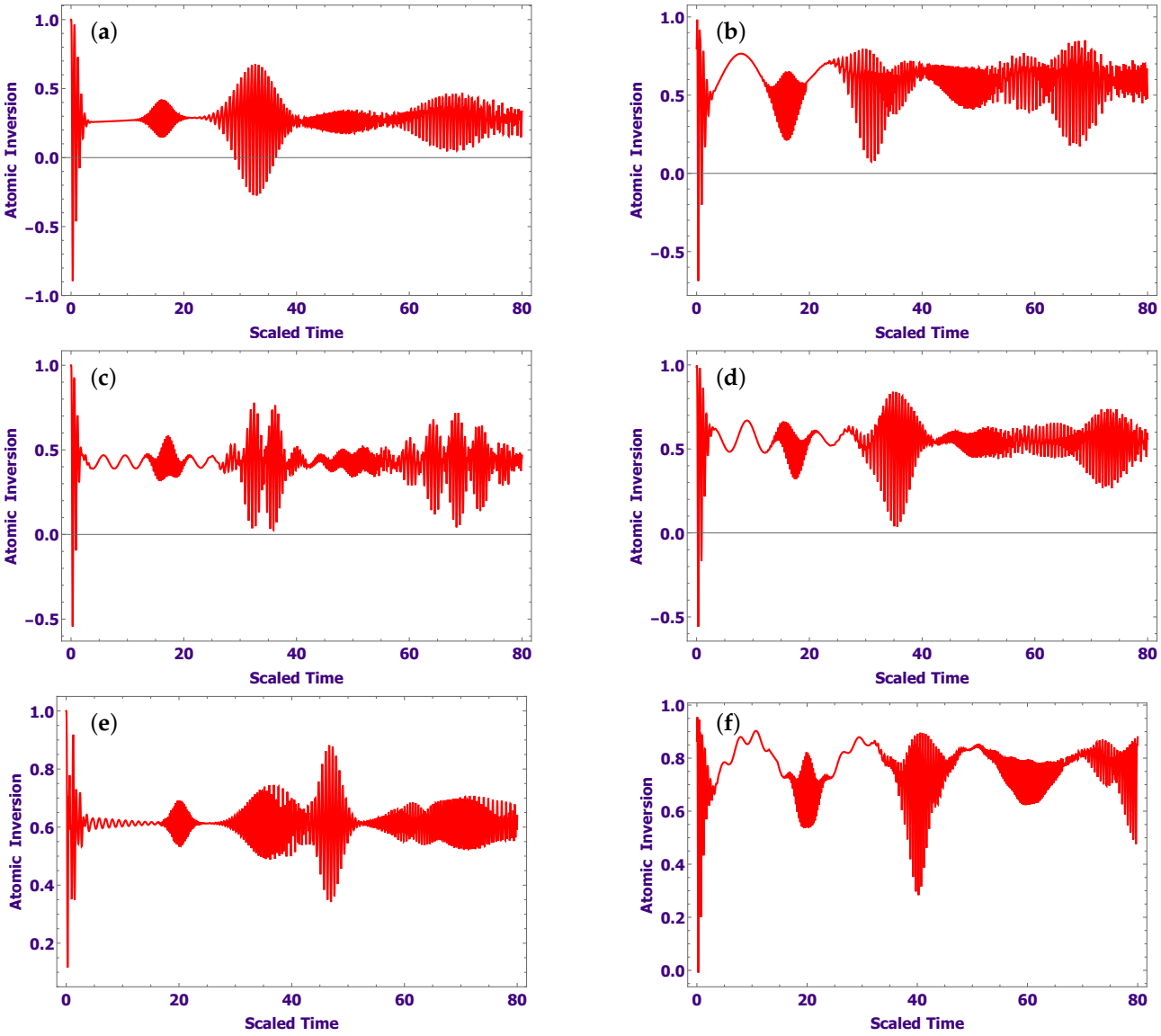

Figure 3. Influence of detuning and external field on population inversion against the scaled time $\lambda_1 t$, (**a**–**f**) the same as Figure 2.

4. Linear Entropy

Linear entropy is one of the best and simplest quantifiers to calculate mixedness and purity degree. For a pure state, the degree of linear entropy is zero, but it has a maximum value for a maximally mixed state. This was derived for an arbitrary quantum state based on purity $\mathcal{P} \equiv -Tr(\rho^2)$ as [38],

$$\mathcal{S}_L(t) = \frac{\mathcal{D}}{\mathcal{D}-1}\left(1 - Tr(\rho_A^2)\right) \tag{20}$$

where $\mathcal{D}$ is the dimension of atomic subsystem. By employing the wavefunction (10), one can obtain explicitly the linear entropy of the atomic state as follows:

$$\mathcal{S}_L(t) = \frac{4}{3}\left(1 - \sum_{i,j=1,i\neq j}^{4}(\rho_{ii} + 2\rho_{ij}\rho_{ji})\right) \tag{21}$$

As displayed in Figure 4, the degree of mixedness and purity via linear entropy is related to the collapse–revival phenomenon. In the absence of the effect of the classical field with a small detuning, Figure 4a shows that the mixedness increases after the onset interaction between atom and field. As shown in Figure 4b, where a small effect of the classical field and detuning are added, the mixedness increases as the scaled time increases, and decreases once the atom–field interaction collapses. The external field increases the lower bounds of the linear entropy; hence, the purity of the system increases. As the detuning parameters increase $(\delta_1, \delta_2, \delta_3) = (6\omega_f, 3\omega_f, 6\omega_f)$ with $(\lambda_2 = 0)$, the maximum bounds of linear entropy decrease. Therefore, the purity of the atomic state increases. By taking the effect of the classical field into our account $(\lambda_2 = 0.3)$, the maximum bounds of linear entropy grow as the scaled time increases. Additionally, the amplitudes of the osculation increase. At robust detuning and deficiency of the classical field, the upper bounds of linear entropy between the atom and field decrease, while the lower bounds increase. This means that the purity of the system increases by increasing the detuning. Nevertheless, the intense external classical field enhances the lower bounds of the purity and grows the upper bounds as dimensionless time grows. Overall, the destructive influence of the external field parameter may be resisted by raising the intensity of the detuning parameter. Furthermore, at higher values of the classical field parameter, purity is weak at high detuning, where the upper bounds of their amplitudes are extending.

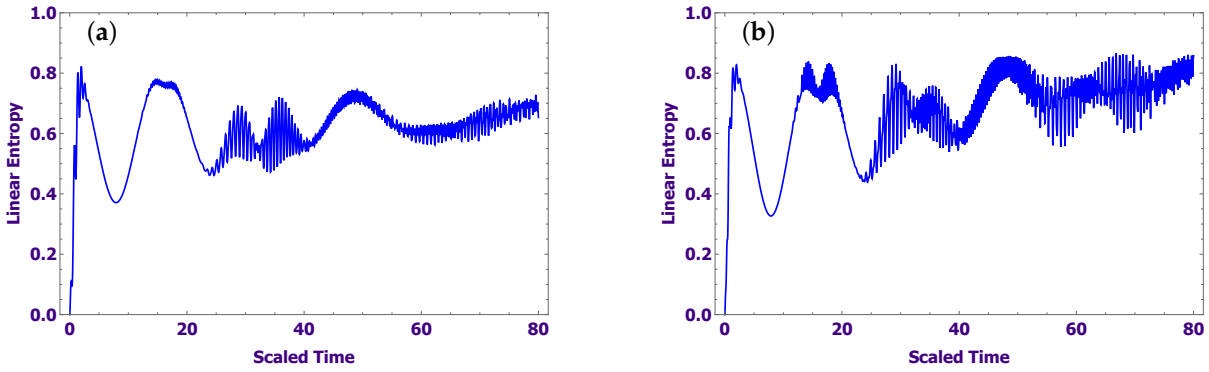

Figure 4. *Cont.*

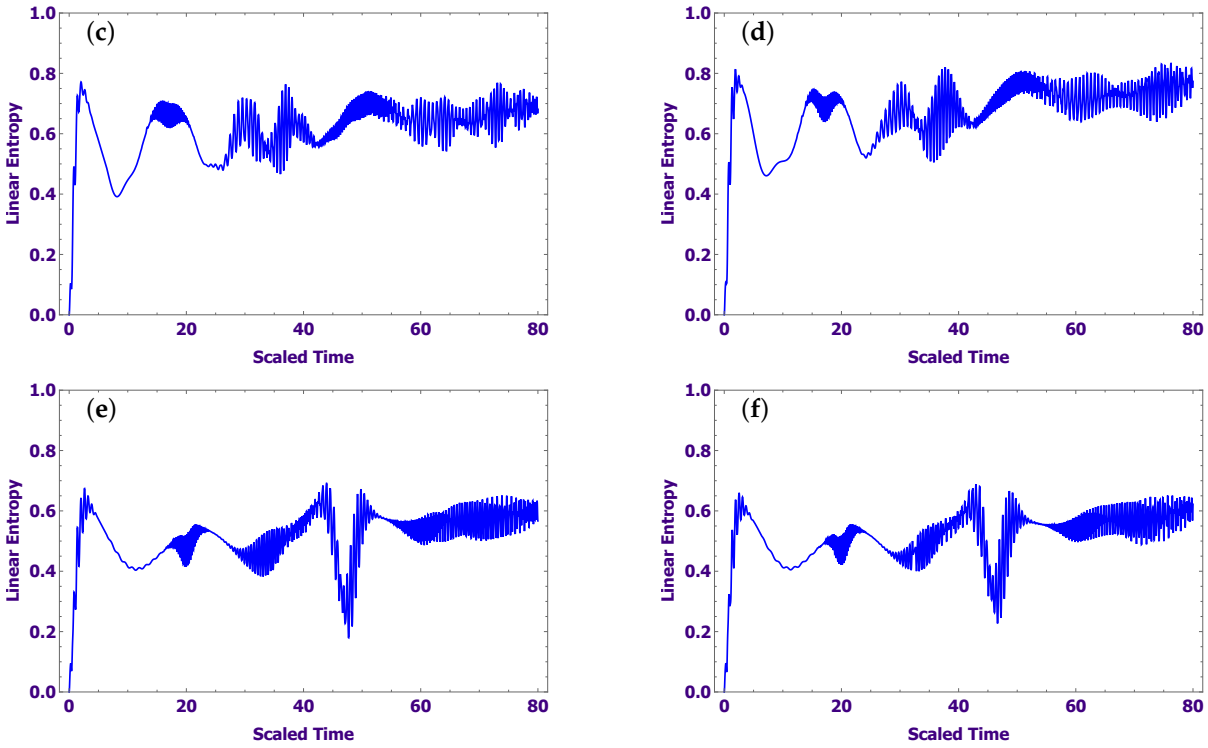

Figure 4. Influence of detuning and external field on degree mixedness against the scaled time $\lambda_1 t$, (**a**–**f**) with the same as Figure 2.

5. l_1 Norm of Coherence

The l_1 norm of coherence is one of the most common quantifiers of quantum coherence. In the first place, it is a geometric (distance) measure, where it is defined as the sum of the magnitudes of all off-diagonal entries. The l_1 norm of coherence for a quantum state $\rho = \sum_{a,b} \rho_{a,b} |a\rangle\langle b|$ has the following form [31],

$$\mathcal{C}_{l_1} = \sum_{a \neq b} |\rho_{a,b}|, \tag{22}$$

where $\rho_{a,b}$ denotes all the off-diagonal elements of the total density operator.

In Figure 5, we discuss the influence of external classical fields and detuning parameters on the degree of coherence by using the l_1 norm of coherence. The general behavior of quantum coherence indicates that the function $\mathcal{C}_{l_1}$ oscillates proportionally to the statistical population inversion. It is clear that the detuning and the classical field parameters play as control rules for minimizing or maximizing the coherence degree. In general, the numerical behavior of coherence degree for large and small detuning at the onset interaction is zero. In the presence of the classical field, the coherence at the onset interaction is 0.6, 0.1, or 0.5 depending on the strength of detuning. The minimum bounds of quantum coherence are enhanced as the intensity of the classical field increases, while the maximum bounds decrease. This means that by controlling the classical field parameter, one can improve the possibility of restringing the decoherence of the system induced by the detuning parameter.

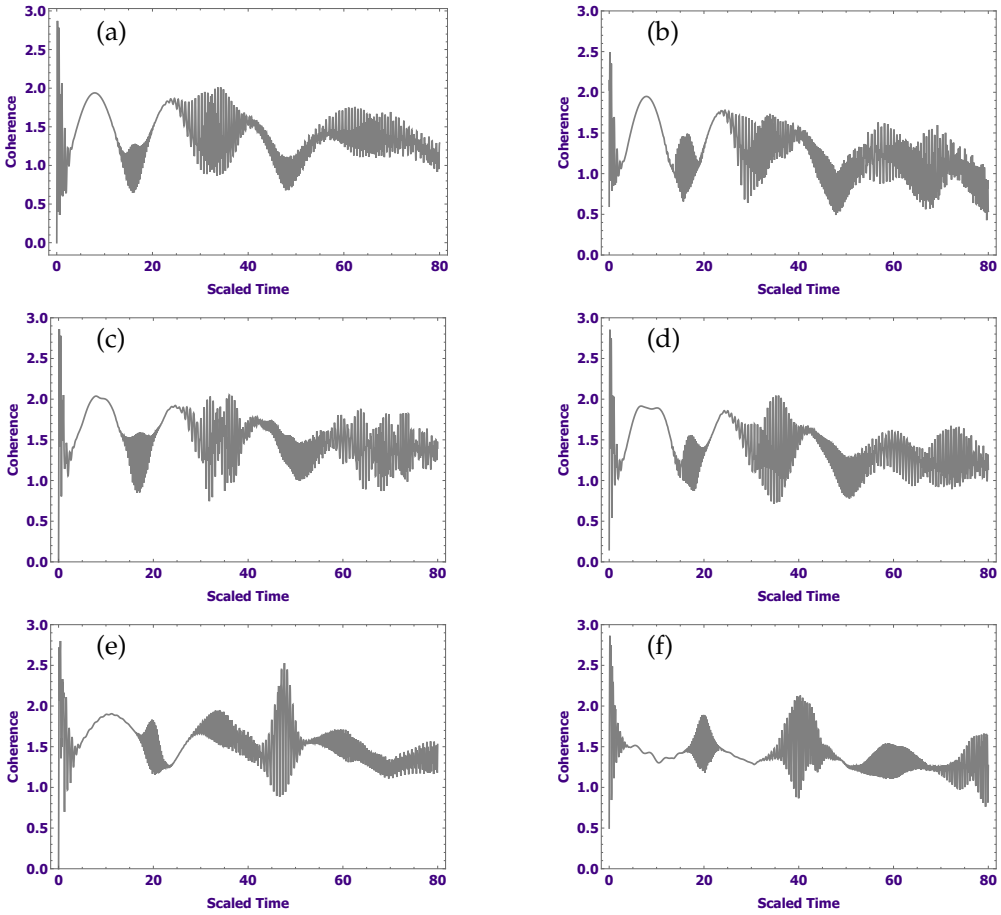

Figure 5. Influence of detuning and external field on degree coherence against the scaled time $\lambda_1 t$, (**a**–**f**) the same as Figure 2.

6. Conclusions

A quantum system consists of a single ◊-configuration four-level atom that interacts locally with a single-mode quantized cavity field. It is assumed that the initial cavity field is in the coherent state while the atomic system is in the upper state. The exact solution of the Schrödinger equation under some canonical conditional of dressed states is solved. These new states allow us to find a solution without taking any approximations into account. We discuss the effect of the detuning parameter and external classical field on the behavior of atomic levels, mixedness and coherence. Our results show that the maximum bounds of the occupation of atomic levels depend on the strength of the classical field and the detuning parameters. The classical field parameter reduces the energy of the lower state, and increases the maximum bounds of the upper state.

We discuss the influence of the detuning parameter on the behaviors of the statistical inversion, the mixedness and the coherence. It is shown that the decreasing rate of the three phenomena depend on detuning. The lower bounds of statistical inversion and quantum coherence decrease as the detuning parameters increase. However, the maximum bounds of the mixedness degree decrease as the detuning increases, and consequently, the maximum mixed state switches to a mixed or pure state.

The impacts of different values of the external classical field on the general behaviors of the three phenomena in the presence of detuning parameters are investigated. It is depicted that the destruction induced by the detuning parameters may be resisted by raising the strength of the classical field parameter. At large values of the classical field, the purity is weak, with high detunings, where amplitudes are extending. The lower bounds of coherence are improved as the classical field increases. Therefore, by controlling the classical field parameter, one can improve the possibility of restringing the decoherence

of the system. Finally, the intensity of the external classical field may be considered to be a control parameter that maximizes or minimizes the temporal evolution of mixedness and coherence.

Author Contributions: E.M.K. is responsible for providing methodology, proofs, writing—review and editing. and H.A.-Z. is responsible for review and editing, M.Y.A.-R. is responsible for software, investigation, writing—first draft. All authors have read and agreed to the published version of the manuscript.

Funding: This Research was supported by Taif University Researchers Supporting Project Number (TURSP-2020/17), Taif University, Taif, Saudi Arabia.

Institutional Review Board Statement: Not applicable.

Informed Consent Statement: Not applicable.

Data Availability Statement: Not applicable.

Acknowledgments: This Research was supported by Taif University Researchers Supporting Project Number (TURSP-2020/17), Taif University, Taif, Saudi Arabia. So the authors are thankful of Taif university for this support. Thanks of cooperation's.

Conflicts of Interest: The authors declare no conflict of interest.

References

1. Rabi, I.I. Space quantization in a gyrating magnetic field. *Phys. Rev.* **1937**, *51*, 652–654. [CrossRef]
2. Jaynes, E.T.; Cummings, F.W. Comparison of quantum and semiclassical radiation theories with application to the beam maser. *Proc. IEEE* **1963**, *51*, 89–109. [CrossRef]
3. Abdel-Hafez, A.M.; Abu-Sitta, A.M.M.; Obada, A.-S.F. A generalized Jaynes- Cummings model for the N-level atom and (N- 1) modes. *Physica A* **1989**, *156*, 689–712. [CrossRef]
4. Skrypnyk, T. The N-level, N- 1-mode Jaynes-Cummings model: Spectrum and eigenvectors. *J. Phys. A* **2013**, *46*, 052001. [CrossRef]
5. Abdel-Hafez, A.M.; Obada, A.-S.F. Amplitude-squared squeezing in the multiphoton Jaynes-Cummings model: Effect of phases. *Phys. Rev. A* **1991**, *44*, 6017–6022. [CrossRef]
6. Abdel-Khalek, S.; Khalil, E.M.; Alotaibi, H.; Abo-Dahab, S.M.; Mahmoud, E.E.; Higazy, M.; Marin, M. Effects of energy dissipation and deformation function on the entanglement, photon statistics and quantum fisher information of three-level atom in photon-added coherent states for morse potential. *Symmetry* **2021**, *13*, 2188. [CrossRef]
7. Salah, A.; Thabet, L.E.; El-Shahat, T.M.; El-Wahab, N.H.A. On the interaction between tripod-type four-level atom and one-mode field in the presence of a classical homogeneous gravitational field. *Pramana* **2020**, *94*, 143. [CrossRef]
8. Obada, A.-S.F.; Ahmed, M.M.A.; Farouk, A.M. The dynamics of a five-level (double λ)-type atom interacting with two-mode field in a cross Kerr-like medium. *Int. J. Theor. Phys.* **2018**, *57*, 1210–1223. [CrossRef]
9. Baghshahi, H.R.; Tavassoly, M.K.; Behjat, A. Entanglement of a damped non-degenerat $\Diamond$-type atom interacting nonlinearly with a single-mode cavity. *Eur. Phys. J. Plus* **2016**, *131*, 80. [CrossRef]
10. Zidan, N.; Abdel-Hameed, H.F.; Metwally, N. Quantum Fisher information of atomic system interacting with a single cavity mode in the presence of kerr medium. *Sci. Rep.* **2019**, *9*, 2699. [CrossRef]
11. Liao, Q.; He, G. Maximal entanglement and switch squeezing with atom coupled to cavity field and graphene membrane. *Quantum Inf. Process.* **2020**, *19*, 91. [CrossRef]
12. Alotibi, M.F.; Khalil, E.M.; Abdel-Khalek, S.; Abd-Rabbou, M.Y.; Omri, M. Effects of the vibrating graphene membrane and the driven classical field on an atomic system coupled to a cavity field. *Results Phys.* **2021**, *31*, 105012. [CrossRef]
13. Abdalla, M.S.; Khalil, E.M.; Obada, A.S.-F. Exact treatment of the Jaynes-Cummings model under the action of an external classical field. *Ann. Phys.* **2011**, *326*, 2486–2498. [CrossRef]
14. Metwally, N.; Hassan, S.S. Estimation of pulsed driven qubit parameters via quantum Fisher information. *Laser Phys. Lett.* **2017**, *14*, 115204. [CrossRef]
15. Abd-Rabbou, M.Y.; Khalil, E.M.; Ahmed, M.M.A.; Obada, A.S.F. External classical field and damping effects on a moving two level atom in a cavity field interaction with Kerr-like medium. *Int. J. Theor. Phys.* **2019**, *58*, 4012–4024. [CrossRef]
16. Metwally, N. Dynamics of information in the presence of deformation. *Int. J. Quantum Inf.* **2011**, *9*, 937–946. [CrossRef]
17. Altowyan, A.S.; Abdel-Khalek, S.; Berrada, K. Emission spectrum and geometric phase in deformed Jaynes-Cummings model. *Results Phys.* **2020**, *16*, 102924. [CrossRef]
18. Shen, J.-Q.; Ruan, Z.-C.; He, S. Influence of the signal light on the transient optical properties of a four-level EIT medium. *Phys. Lett. A* **2004**, *330*, 487–495. [CrossRef]
19. Abdel-Wahab, N.H. General formalism of the interaction of a single-mode cavity field with a four-level atom. *Eur. Phys. J. Plus* **2011**, *126*, 1–10. [CrossRef]

20. Sheng, J.; Yang, X.; Khadka, U.; Xiao, M. All-optical switching in an N-type four-level atom-cavity system. *Opt. Express* **2011**, *19*, 17059–17064. [CrossRef]
21. Yu-Yuan Chen, Ya-Nan Li, and Ren-Gang Wan. Double-cavity optical bistability and all-optical switching in four-level N-type atomic system. *JOSA B* **2018**, *35*, 1240–1247. [CrossRef]
22. Parvaz, M.; Askari, H.R.; Baghshahi, H.R. Mechanical squeezing of the tripod-type four-level atom-assisted optomechanical system. *Phys. Scr.* **2019**, *94*, 125105. [CrossRef]
23. Obada, A.-S.F.; Khalil, E.M.; Ahmed, M.M.A.; Elmalky, M.M.Y. Influence of an external classical field on the interaction between a field and an atom in presence of intrinsic damping. *Int. J. Theor. Phys.* **2018**, *57*, 2787–2801. [CrossRef]
24. Obada, A.-S.F.; Alshehri, N.A.; Khalil, E.M.; Abdel-Khalek, S.; Habeba, H.F. Entropy squeezing and atomic Wehrl density for the interaction between SU(1, 1) Lie algebra and a three-level atom in presence of laser field. *Results Phys.* **2021**, *30*, 104759. [CrossRef]
25. Coffman, V.; Kundu, J.; Wootters, W.K. Distributed entanglement. *Phys. Rev. A* **2000**, *61*, 052306. [CrossRef]
26. Horodecki, R.; Horodecki, P.l.; Horodecki, M.l.; Horodecki, K. Quantum entanglement. *Rev. Mod. Phys.* **2009**, *81*, 865–942. [CrossRef]
27. Baghshahi, H.R.; Tavassoly, M.K.; Behjat, A. Dynamics of entropy and non-classicality features of the interaction between a ◊-type four-level atom and a single-mode field in the presence of intensity-dependent coupling and Kerr non-linearity. *Commun. Theor. Phys.* **2014**, *62*, 430. [CrossRef]
28. Pan, G.; Xiao, R.; Gao, J. Enhanced entanglement and output squeezing of optomechanical system via a single four-level atom. *Laser Phys. Lett.* **2020**, *17*, 085204. [CrossRef]
29. Anwar, S.J.; Ramzan, M.; Khan, M.K. Dynamics of entanglement and quantum Fisher information for N-level atomic system under intrinsic decoherence. *Quantum Inf. Process.* **2017** *16*, 142. [CrossRef]
30. Anwar, S.J.; Ramzan, M.; Usman, M.; Khan, M.K. Entanglement dynamics of three and four level atomic system under stark effect and kerr-like medium. *Quantum Rep.* **2019**, *1*, 23–36. [CrossRef]
31. Baumgratz, T.; Cramer, M.; Plenio, M.B. Quantifying coherence. *Phys. Rev. Lett.* **2014**, *113*, 140401. [CrossRef] [PubMed]
32. Radhakrishnan, C.; Parthasarathy, M.; Jambulingam, S.; Byrnes, T. Distribution of quantum coherence in multipartite systems. *Phys. Rev. Lett.* **2016**, *116*, 150504. [CrossRef] [PubMed]
33. Streltsov, A.; Singh, U.; Dhar, H.S.; Bera, M.N.; Adesso, G. Measuring quantum coherence with entanglement. *Phys. Rev. Lett.* **2015**, *115*, 020403. [CrossRef] [PubMed]
34. Winter, A.; Yang, D. Operational resource theory of coherence. *Phys. Rev. Lett.* **2016**, *116*, 120404. [CrossRef] [PubMed]
35. Zhong, P.-G.; Li, C.; Wang, Y.; Song, J.; Liu, S.-T.; Jiang, Y.-Y.; Xia, Y. Quantum phase transitions triggered by a four-level atomic system in dissipative environments. *Phys. Rev. A*. **2019**, *99*, 043829. [CrossRef]
36. Wen, F.; Zheng, H.; Xue, X.; Chen, H.; Song, J.; Zhang, Y. Electromagnetically induced transparency-assisted four-wave mixing process in the diamond-type four-level atomic system. *Opt. Mater.* **2014**, *37*, 724–726. [CrossRef]
37. Li, S.; Yang, X.; Cao, X.; Zhang, C.; Xie, C.; Wang, H. Enhanced Cross-Phase Modulation Based on a Double Electromagnetically Induced Transparency in a Four-Level Tripod Atomic System. *Phys. Rev. Lett.* **2008**, *101*, 073602. [CrossRef]
38. Wei, T.C.; Nemoto, K.; Goldbart, P.M.; Kwiat, P.G.; Munro, W.J.; Verstraete, F. Maximal entanglement versus entropy for mixed quantum states. *Phys. Rev. A* **2003**, *67*, 022110. [CrossRef]